Reconfigurable Memristive Pulse Generator based on Pulse Shaping for Ultra-Wideband Communication

Imen Barraj
Department of Computer Engineering, College of Computer Engineering and Sciences, Prince Sattam bin Abdulaziz University, Al-Kharj 11942, Saudi Arabia
i.barraj@psau.edu.sa (corresponding author)

Amel Neifar
Systems Integration & Emerging Energies (SI2E), Electrical Engineering Department, National Engineering School of Sfax, University of Sfax, Sfax, Tunisia
amel.neifar@enis.tn

Hassen Mestiri
Department of Computer Engineering, College of Computer Engineering and Sciences, Prince Sattam bin Abdulaziz University, Al-Kharj 11942, Saudi Arabia
h.mestiri@psau.edu.sa

Mohamed Masmoudi
Systems Integration & Emerging Energies (SI2E), Electrical Engineering Department, National Engineering School of Sfax, University of Sfax, Sfax, Tunisia
mohamed.masmoudi@enis.tn

Received: 29 November 2024 | Revised: 24 December 2024 and 1 January 2025 | Accepted: 6 January 2025

 DOI: https://doi.org/10.48084/etasr.9771

ABSTRACT

This paper presents a novel reconfigurable memristive Pulse Generator (PG) designed for Ultra-Wideband (UWB) applications, leveraging the advanced pulse shaping techniques. The proposed design aims to improve the efficiency and flexibility of UWB communication systems, thereby contributing to the achievement of the "Sustainable Development Goal 9: Industry, Innovation, and Infrastructure" by promoting technological advances in the field of communications. The design utilizes the CMOS 0.18 µm technology operating at 1.8 V to achieve high performance and low power consumption. By employing constant resistance and dynamic resistance modulation, the proposed PG supports various modulation schemes, including Frequency-Shift Keying (FSK) and On-Off Keying (OOK), enhancing its adaptability and efficiency. The transmitter demonstrates significant energy efficiency with a low-duty cycle impulse approach, operating within the lower UWB band (3-5 GHz) to minimize interference. The simulation results indicate that the UWB generator achieves high data rates and improved spectral efficiency while maintaining compliance with the FCC regulations. This makes it ideal for integration into IoT devices, wearable technology, and other battery-powered applications. Therefore, the proposed design has the potential to enhance connectivity and data transmission capabilities, ultimately supporting the development of more efficient and reliable communication networks worldwide.

Keywords-pulse generator; memristor; ultra-wideband; shape filter; wireless communication

I. INTRODUCTION

Memristors were first theorized by Leon Chua in 1971 and later developed and experimentally demonstrated by Hewlett-Packard Laboratories in 2008 [1]. These devices provide variable resistance, allowing for efficient information storage by transitioning between low and high resistance states. Memristors are characterized by their unique pinched hysteresis loop, which shows the relationship between the applied voltage and the resulting current. This loop indicates the memristor's ability to "remember" its resistance state, even after the power is turned off [1-2]. This property makes

memristors promising for use in various applications, such as non-volatile memory, neural networks, and reconfigurable electronics. Researchers continue to explore the potential of memristors to develop new design architectures for more energy-efficient and reliable devices with improved performance and functionality. One area of interest is the use of memristors in analog designs to create more efficient and adaptive circuits [3-6]. This paper explores the potential advantages of integrating memristors into UWB designs, emphasizing their ability to improve performance and flexibility.

The PG circuit is a critical component in UWB systems, and the integration of memristors could potentially enhance its functionality by allowing for more precise control over pulse generation and timing [7-9]. In addition, the use of memristors in UWB designs can also lead to reduced power consumption and improved signal quality, making it a promising technology for future wireless communication systems. Therefore, a memristor-based reconfigurable PG is proposed in this work. The PG operates within the 3–5 GHz frequency band and utilizes a pulse shaping approach. Additionally, it enables the generation of various UWB wavelets with spectrum tunability. This novel approach offers flexibility in designing pulse shapes tailored to specific communication requirements.

II. PROPOSED UWB PULSE GENERATOR

UWB PGs were initially designed using discrete components, such as tunnel diodes, step recovery diodes, and nonlinear transmission lines [10]. These designs offered high peak amplitude but consumed more power and occupied large areas. However, advances in technology have led to the development of integrated circuit solutions for UWB pulse generation that offer improved performance and reliability. These integrated solutions also provide a more compact and cost-effective alternative to traditional discrete component designs. The design techniques for CMOS PGs can be categorized into several types: digitally delayed positive and negative peak impulse combination [11], oscillator-based PGs [12], the derivative of pulse rising and falling edges [13], and spectrum filtering [14]. Each of these design techniques has its own advantages and limitations. The digitally delayed positive and negative peak impulse combination offers precise control over the pulse width and amplitude, making it ideal for applications requiring high accuracy. However, this technique can be more complex to implement than other design methods. Oscillator-based PGs are simpler to implement and provide a stable output frequency but may have limitations in terms of the pulse width control. The derivative of pulse rising and falling edges provides a way to achieve fast rise and fall times in the generated pulses but can be more complex to implement. Spectrum filtering is effective in reducing noise and harmonics in the output signal but may require additional components for implementation. Each design technique should be carefully considered based on the specific requirements of the application.

The generator proposed in this work utilizes an oscillator-based design. The use of memristors will address the issue of pulse width limitation. Memristors will enable a precise control of the pulse width and shape, leading to improved performance and flexibility in a wide range of applications. Additionally, the use of memristors can help reduce the power consumption and improve the overall efficiency of the generator design. Figure 1 illustrates the proposed design for a memristive UWB reconfigurable PG, comprising a Memristive Switchable Ring Oscillator (MS-RO), a control circuit, and a Pulse Shaping Filter (PSF). The MS-RO provides frequency tuning, whereas the control circuit ensures precise timing, synchronization, and dynamic reconfiguration of the pulse characteristics. The PSF further refines the output signal to meet the UWB specifications and ensure optimal performance.

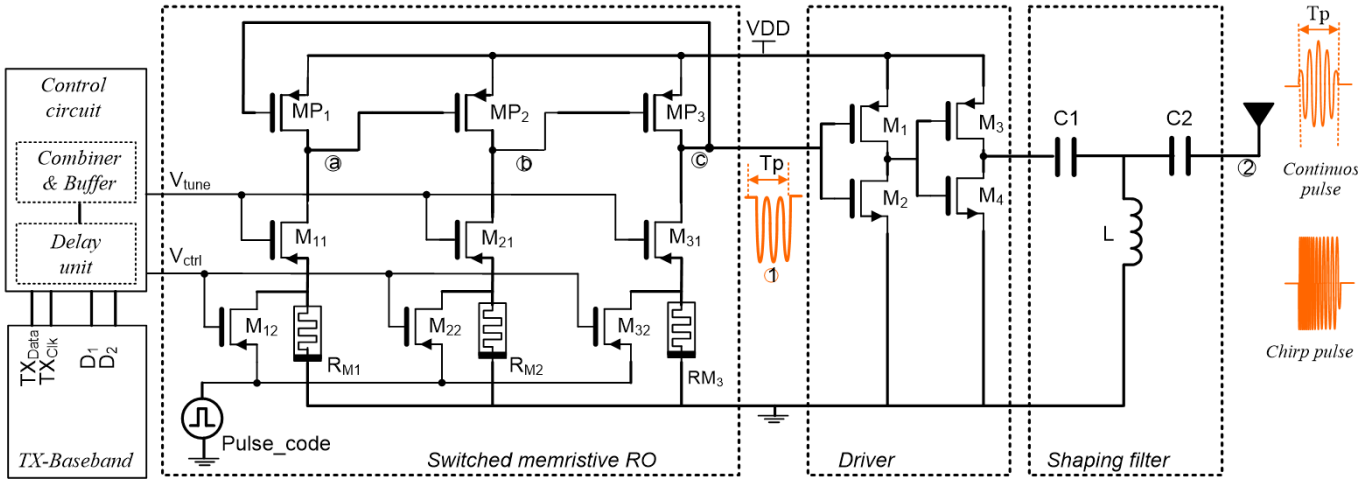

Fig. 1. Proposed memristor based reconfigurable PG.

The MS-RO, designed with three-stage memristive PMOS Inverters (M-Inv), leverages the unique properties of memristors to create a stable and reliable oscillator. This design ensures proper amplification and feedback, which are crucial for maintaining the desired frequency and duty cycle of the output pulses. By integrating memristors, the M-Inv takes advantage of their non-volatility and low power consumption to generate controllable pulses with a defined shape. It consists

of a PMOS transistor connected in series with a memristor. The memristor, acting as a variable resistor, regulates the timing and amplitude of the output pulses. This setup enables accurate control of the current passing through the PMOS transistor, thereby shaping the output waveform. The NMOS transistors M_{11}, M_{21}, and M_{31} regulate the connections between the memristors R_{M1}, R_{M2}, and R_{M3} and the PMOS transistors MP_1, MP_2, and MP_3, respectively. The control signal V_{tune} controls the operation mode of these transistors. This configuration allows a precise control of the current flow through the memristors, enabling efficient data storage and retrieval. The PMOS transistors act as switches to regulate the current flow through the memristors based on the input signals received. As depicted in Figure 1, each memristor is connected to its programming circuit, comprising an NMOS transistor that is regulated by the control signal V_{prog}. When activated, the NMOS transistor allows the memristor to be programmed by applying a specific voltage or current pulse. This programming process alters the resistance state of the memristor, which is then stored as data. Overall, this configuration ensures reliable and accurate data storage and retrieval within the system. The driver, consisting of two inverter stages (transistors M_1–M_4), amplifies the signal produced at its input while also isolating the MS-RO from the PSF load. This topology was chosen for its low complexity, minimal area requirement, and negligible power consumption.

The PSF consists of passive components that manipulate the waveform by altering its amplitude, rise time, and fall time. The use of passive components in the PSF also contributes to minimizing the power consumption and maintaining signal integrity throughout the process. The control circuit is crucial for the proper synchronization and modulation of signals within the generator. It combines different input signals using voltage-controlled delay lines, CMOS edge combiners, and logic gates to generate the required control signals (V_{tune} and V_{prog}). The integration of these components allows for precise timing and coordination of signals, resulting in the smooth and reliable operation of the generator.

III. OPERATING SCENARIOS

There are two operating scenarios for controlling memristor resistance during oscillations. The first scenario involves constant resistance control, where the memristor's resistance stays unchanged during the oscillation process. In this case, the generator can produce a wideband spectrum with fewer oscillations per pulse or a narrowband spectrum with more oscillations. This choice between wideband and narrowband spectra provides flexibility to meet various communication requirements, thereby allowing the proposed design to adapt to a variable spectrum power. The second scenario uses dynamic resistance modulation. Here, the memristor's resistance varies with the fluctuating current levels, leading to oscillations with a variable frequency over time that generate chirp pulses. These pulses can be used for radar applications as the changing frequency enhances target detection and tracking. Additionally, it offers a more effective way to control the generator's spectrum power output, accommodating different modulation types, such as FSK and OOK. The generation of oscillations in the two modes goes through four phases: initialization, programming, operation, and reset.

A. Constant Resistance Control

During the programming phase, transistors M_{11}, M_{21}, and M_{31} are off, whereas transistors MP_{1-3} operate in the subthreshold region, generating no output signal. The feedback node bias is set to zero and the buffer is disabled to ensure proper pulse generation. The R_m value is adjusted by activating transistors M_{12}, M_{22}, and M_{32} and connecting the R_m terminals to the input pulse code and ground. Once the desired R_m value is reached, M_{12}, M_{22}, and M_{32} are turned off and M_{11}, M_{21}, and M_{31} are turned on, connecting the adjusted R_m to the MP_{1-3} transistors, and initiating the operating phase. During the operation phase, the MS-RO gain stage nodes are biased to a voltage dependent on the PMOS size ratio, ensuring optimal signal amplification. This bias disrupts the oscillation start, activating the buffer and leading to rapid oscillations that generate a stable output signal. The control signal V_{tune} activates the MS-RO for a duration equal to the pulse period, adjusting frequency and amplitude to maintain stability. The MS-RO efficiently converts the baseband signal V_{tune} to a wideband RF signal, meeting the FCC spectral mask requirements using PSF to reduce spectrum sidelobes. In the reset phase, the MS-RO and buffers are disabled, stopping oscillation rapidly and reducing the power consumption. The M_{12}, M_{22}, and M_{32} transistors are activated, connecting R_m to the negative input pulse code, ensuring proper initialization for the next input pulse. The MS-RO generates pulses of variable frequency and width, offering high precision and stability, and can be easily integrated into the existing systems, making it suitable for various applications.

B. Dynamic Resistance Modulation

During the first initialization phase, the MS-RO circuits are initialized to ensure stability and prevent potential issues during the duty cycle. In the memristance programming phase, a positive pulse code programs the memristance to the desired resistance state, R_{fh}, determining the chirp pulse high sub-band frequency, ensuring precise control, and optimal frequency allocation for reliable communication. The frequency ramping phase involves maintaining the voltage at the memristor terminals above the threshold to tune memristance over time, generating chirped pulse signals. This phase ends when the desired lower sub-band frequency is achieved and determines the chirp pulse width, which is critical to signal resolution and accuracy. The second initialization phase involves enabling the MS-RO and using a negative pulse code to reset the memristance value to R_{on}, ensuring that the MS-RO is ready for accurate data transmission.

IV. SIMULATION RESULTS AND DISCUSSION

The UWB tunable memristive transmitter, designed using the TSMC CMOS 0.18 µm technology and operating at 1.8 V, delivers high performance with low power consumption. This work integrated memristors with the TSMC CMOS 0.18 µm technology by employing the VTEAM memristor model, implemented in Verilog-A using the Advanced Design System (ADS) tool. This approach allowed performing comprehensive simulations of the electrical circuit performance. As a result,

this combination is highly efficient and well-suited for advanced wireless communication applications. Designed to drive a 50 Ω UWB single-ended antenna, the transmitter ensures efficient signal transmission and reception.

In the case of constant resistance control, it employs the OOK modulation for efficient and cost-effective data transmission in wireless communication systems. The transmitter's compatibility with non-coherent energy detector receivers simplifies the system design and reduces cost. Operating at 10 MHz Pulse Repetition Frequency (PRF) with a low-duty cycle impulse approach, it demonstrates significant energy efficiency within the lower UWB band (3-5 GHz), which is less crowded. The transmitter can operate in two modes: multiband and monoband. In the multiband mode, it dynamically switches between different frequency bands within the lower UWB band, enhancing communication flexibility and system performance by adapting to varying environmental conditions. It covers the three low bands of the IEEE 802.15.4a standard with a bandwidth of 500 MHz. In the monoband mode, it operates on a single fixed frequency within the lower UWB band with a bandwidth of 1.8 GHz, offering a simpler implementation for applications that do not require frequency agility.

Figure 2 displays the transient response of the MS-RO. As demonstrated during the programming phase, the memristance is adjusted to achieve the desired value, and during the operating phase, this value is maintained constant. This stability in memristance during operation is crucial for the proper functioning of the MS-RO circuit.

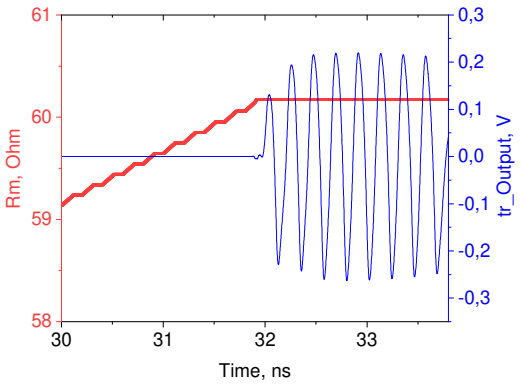

Fig. 2. Transient response of the MS-RO.

The simulation results for this scenario show that the number of oscillations per pulse at the transmitter output can adjust the emitted Power Spectral Density (PSD). By controlling the pulse shaping and modulation techniques, the PSD can be spread over a wider frequency range, enhancing the spectral efficiency, or concentrated within a narrower band for better bandwidth utilization. This balance is crucial for optimizing the power efficiency and spectral limits of narrow and wideband signals. Reducing the number of oscillations per pulse spreads the emitted PSD over a wider frequency range, enhancing the spectral efficiency. Conversely, increasing the number of oscillations concentrates the PSD within a narrower frequency band, optimizing bandwidth utilization. This relationship is crucial for balancing the power efficiency and spectral characteristics in both narrowband and wideband signals, enabling fine-tuning to achieve the desired transmission performance. Adjusting the V_{ctrl} high voltage width allows the fine-tuning of the signal to meet the regulatory requirements or optimize performance in different environments.

Figures 3 and 4 present the transient and frequency response of the proposed design for the multiband and monoband transmission. For the multiband transmission, the uniform pulse duration across channels ensures reliable communication across the low-band spectrum. The PSD spectrum can be adjusted to cover the UWB low band (3-5 GHz) for the IEEE 802.15.4a standard (Band-1, Band-2, Band-3). This design enables seamless transition between different frequency bands, maximizing efficiency and performance in a variety of communication scenarios. Additionally, the flexibility in adjusting the PSD spectrum provides versatility for adapting it to different standards and requirements within the UWB low band. To cover the 500 MHz bandwidth, the oscillation width is 1.75 ns. For monoband transmission, the simulation shows a 0.8 ns pulse width and a 2 GHz -10 dB bandwidth, with the PSD falling below the FCC limits, demonstrating regulatory compliance.

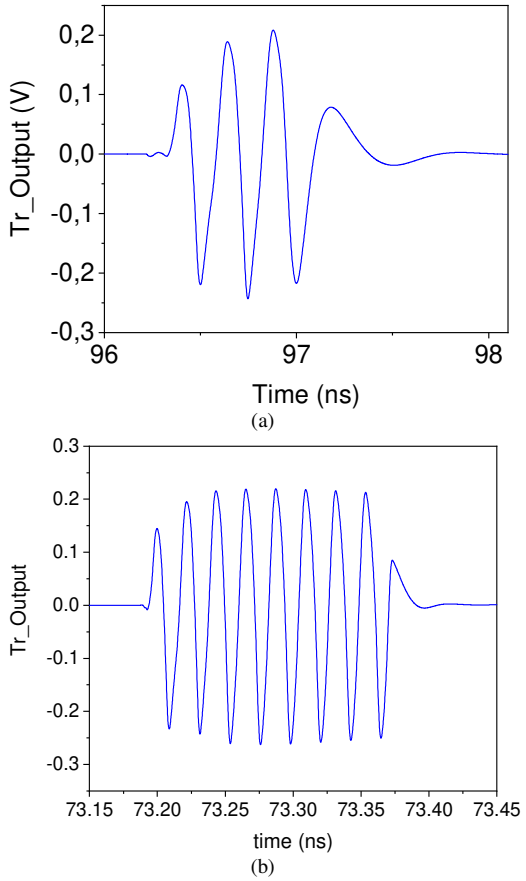

Fig. 3. MS-RO output for (a) monoband transmission and (b) multiband transmission.

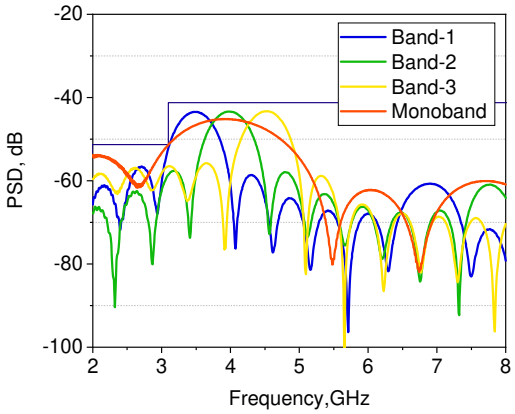

Fig. 4. Frequency response of the MS-RO for constant resistance control approach.

In the second scenario, dynamic resistance modulation combined with the FSK and OOK modulation schemes significantly boosts the transmitter's cost-effectiveness and feasibility. This approach ensures compatibility with the modern integrated circuit manufacturing processes, rendering it a practical choice for modern wireless communication systems. The FSK transmitter uses a modulation scheme in which data bits '0' and '1' are transmitted using two distinct channels, Band0 and Band1, each with a bandwidth of 500 MHz. This setup ensures reliable and efficient transmission within the 3-5 GHz frequency range. Specifically, Band0 (3.2–3.7 GHz) and Band1 (4.1–4.6 GHz) correspond to data bits '0' and '1', respectively. Transient simulations reveal the behavior of the transmitter when sending data bits '1' and '0'. As portrayed in Figure 5, the linear variation of memristance over time generates a chirp pulse at the output. For Band1, the upper and lower frequencies are determined by R_m values between 55 Ω and 120 Ω, requiring a 20 ns chirp pulse width to achieve a 500 MHz bandwidth at -10 dB. Similarly, for Band0, R_m ranges from 157 Ω to 288 Ω, again requiring a 20 ns chirp pulse width for the same bandwidth. These frequency ranges and pulse widths are essential for accurate data transmission, with the chirp pulse exhibiting a peak-to-peak amplitude of 460 mV.

For the OOK modulation schema, the chirped transmitter's pulse width of 50 ns and a peak-to-peak voltage (V_{pp}) of 465 mV ensure precise timing and efficient data transmission. Transient response simulations demonstrate that tuning R_m between 55 Ω and 310 Ω achieves the target frequencies of 3.1 GHz and 4.8 GHz at a mean PRF of 10 MHz. This confirms the transmitter's ability to operate within the UWB low-band spectrum. Figure 6 illustrates the simulated PSD of the transmitter for the FSK and OOK modulation schemas, which complies with the UWB average PSD limit of -41.3 dBm/MHz and the FCC UWB emission mask, ensuring regulatory compliance. Table I highlights that most UWB transmitters in the literature use OOK modulation. The proposed memristive transmitter stands out for its lower power consumption while maintaining comparable energy consumption, making it ideal for ultra-low power wireless communication applications. It offers efficient spectrum tunability, enabling adaptation to various frequency bands and modulation schemes, and compensates for process, voltage, and temperature variations.

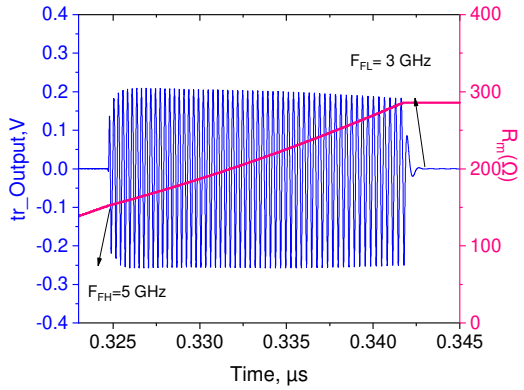

Fig. 5. Transient response of the MS-RO for FSK modulation.

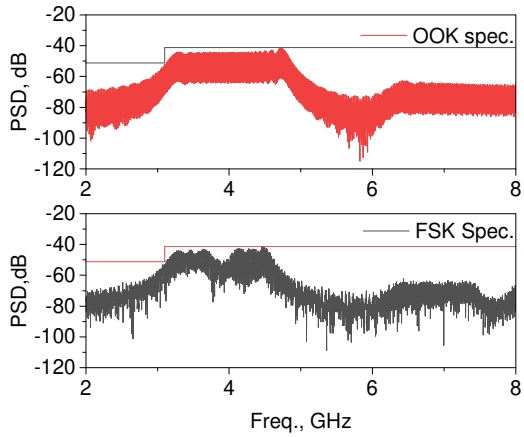

Fig. 6. Frequency response of the MS-RO for the dynamic resistance modulation approach.

TABLE I. PERFORMANCES COMPARISON WITH PREVIOUSLY REPORTED UWB PULSE GENERATORS

Characteristics	[14]	[15]	[16]	[17]	This work
VPP (V)	1.0	0.200	0.130	0.320	0.460
Power cons. (mW)	21.6	10	2.1	1.0	0.094-0.328
Ec (pJ/pulse)	86.0	14.6	27.5	5.0	9.8-16.4
Pulse width (ns)	1.0	-	1.0	0.6	0.8-48
Modulation	BPSK-PAM	OOK	OOK	OOK	FSK-OOK
Bandwidth (GHz)	3.5-6.5	3.75-10.5	3.0-6.0	3.0-7.0	3-5
VDD (V)	1.8	1.8	1.8	1.8	1.8
CMOS (nm)	180	180	180	180	180

The use of memristors in UWB transmitters opens new avenues for enhancing the performance and efficiency of wireless communication systems. Furthermore, the memristive transmitter enables seamless integration with the existing UWB systems, providing a cost-effective solution for upgrading the wireless communication networks. Overall, the incorporation of memristors in UWB transmitters has great potential to

revolutionize the field of ultra-low power wireless communications.

V. CONCLUSION

The reconfigurable memristive Pulse Generator (PG) presented in this paper demonstrates a significant advancement in the design of Ultra-Wideband (UWB) transmitters. By leveraging the CMOS 0.18 µm TSMC technology and dynamic resistance modulation, the proposed design achieves high performance and low power consumption, making it suitable for a wide range of wireless communication applications, including IoT devices and wearable technology. The flexibility in supporting various modulation schemes, such as Frequency-Shift Keying (FSK) and On-Off Keying (OOK), along with efficient spectrum tunability, allows the generator to adapt to different frequency bands and optimize the bandwidth usage. Additionally, the ability to compensate for process, voltage, and temperature variations ensures reliable operation under varying conditions. The simulation results confirm that the proposed design meets the FCC regulatory requirements and achieves high data rates with improved spectral efficiency. Overall, the proposed circuit provides a cost-effective and energy-efficient solution, paving the way for improved performance and efficiency in modern wireless communication systems.

ACKNOWLEDGMENT

The authors extend their appreciation to Prince Sattam bin Abdulaziz University for funding this research work through the project number (PSAU/2024/01/31593)

REFERENCES

[1] D. B. Strukov, G. S. Snider, D. R. Stewart, and R. S. Williams, "The missing memristor found," *Nature*, vol. 453, no. 7191, pp. 80–83, May 2008, https://doi.org/10.1038/nature06932.

[2] L. Chua, "Memristor-The missing circuit element," *IEEE Transactions on Circuit Theory*, vol. 18, no. 5, pp. 507–519, Sep. 1971, https://doi.org/10.1109/TCT.1971.1083337.

[3] I. Barraj, H. Mestiri, and M. Masmoudi, "Overview of Memristor-Based Design for Analog Applications," *Micromachines*, vol. 15, no. 4, Apr. 2024, Art. no. 505, https://doi.org/10.3390/mi15040505.

[4] N. Raj, R. K. Ranjan, and F. Khateb, "Flux-Controlled Memristor Emulator and Its Experimental Results," *IEEE Transactions on Very Large Scale Integration (VLSI) Systems*, vol. 28, no. 4, pp. 1050–1061, Apr. 2020, https://doi.org/10.1109/TVLSI.2020.2966292.

[5] Z. Wu, C. Zhang, J. Zou, C. Peng, and X. Wu, "Threshold Switching Memristor-Based Voltage Regulative Circuit," *IEEE Transactions on Circuits and Systems II: Express Briefs*, vol. 70, no. 3, pp. 1034–1038, Mar. 2023, https://doi.org/10.1109/TCSII.2022.3221140.

[6] Y. Kebbati, P. S. Allaume, and Y. Bennani, "Memristor, Memcapacitor, Meminductor : Models and Experimental Circuit Emulators," *Engineering, Technology & Applied Science Research*, vol. 12, no. 3, pp. 8683–8687, Jun. 2022, https://doi.org/10.48084/etasr.4882.

[7] I. Barraj, M. A. Bahloul, and M. Masmoudi, "Design of 3–5 GHz tunable memristor-based OOK-UWB transmitter," *AEU - International Journal of Electronics and Communications*, vol. 132, Apr. 2021, Art. no. 153664, https://doi.org/10.1016/j.aeue.2021.153664.

[8] J. Lei *et al.*, "Design of a Low-Power, High-Data-Rate, and Crystal-Less All-Digital IR-UWB Transmitter for High-Density Neural Implants," *IEEE Journal of Solid-State Circuits*, vol. 59, no. 7, pp. 2159–2170, Jul. 2024, https://doi.org/10.1109/JSSC.2023.3349077.

[9] A. D. Pitcher, C. W. Baard, and N. K. Nikolova, "Design and Performance Analysis of a Picosecond Pulse Generator," *IEEE Transactions on Instrumentation and Measurement*, vol. 71, pp. 1–14, 2022, https://doi.org/10.1109/TIM.2022.3195265.

[10] J. Han and C. Nguyen, "A new ultra-wideband, ultra-short monocycle pulse generator with reduced ringing," *IEEE Microwave and Wireless Components Letters*, vol. 12, no. 6, pp. 206–208, Jun. 2002, https://doi.org/10.1109/LMWC.2002.1009996.

[11] B. Wei *et al.*, "An all-digital frequency tunable IR-UWB transmitter with an approximate 15th derivative Gaussian pulse generator," *Integration*, vol. 69, pp. 301–308, Nov. 2019, https://doi.org/10.1016/j.vlsi.2019.07.002.

[12] I. Barraj, M. Bahloul, M. E. Fouda, and M. Masmoudi, "Compact memristor-based ultra-wide band chirp pulse generator," *International Journal of Circuit Theory and Applications*, vol. 48, no. 2, pp. 286–293, Feb. 2020, https://doi.org/10.1002/cta.2717.

[13] S. K. Bitra and S. Miriyala, "An Ultra-Wideband Band Pass Filter using Metal Insulator Metal Waveguide for Nanoscale Applications," *Engineering, Technology & Applied Science Research*, vol. 11, no. 3, pp. 7247–7250, Jun. 2021, https://doi.org/10.48084/etasr.4194.

[14] P. Gunturi, N. W. Emanetoglu, and D. E. Kotecki, "A 250-Mb/s Data Rate IR-UWB Transmitter Using Current-Reused Technique," *IEEE Transactions on Microwave Theory and Techniques*, vol. 65, no. 11, pp. 4255–4265, Nov. 2017, https://doi.org/10.1109/TMTT.2017.2695189.

[15] M. Shen, Y.-Z. Yin, H. Jiang, T. Tian, and J. H. Mikkelsen, "A 3–10 GHz IR-UWB CMOS Pulse Generator With 6 mW Peak Power Dissipation Using A Slow-Charge Fast-Discharge Technique," *IEEE Microwave and Wireless Components Letters*, vol. 24, no. 9, pp. 634–636, Sep. 2014, https://doi.org/10.1109/LMWC.2014.2332057.

[16] K. Ture, A. Devos, F. Maloberti, and C. Dehollain, "Area and Power Efficient Ultra-Wideband Transmitter Based on Active Inductor," *IEEE Transactions on Circuits and Systems II: Express Briefs*, vol. 65, no. 10, pp. 1325–1329, Oct. 2018, https://doi.org/10.1109/TCSII.2018.2853190.

[17] J. Radic, M. Brkic, A. Djugova, M. Videnovic-Misic, B. Goll, and H. Zimmermann, "Ultra-low power low-complexity 3–7.5 GHz IR-UWB transmitter with spectrum tunability," *IET Circuits, Devices & Systems*, vol. 14, no. 4, pp. 521–527, 2020, https://doi.org/10.1049/iet-cds.2019.0392.